

## Mild Method for the Agglomeration of Dispersed Polycaprolactone Microspheres via a Genipin-Crosslinked Gelatin Hydrogel

Qingchun Zhang, Yan Zhang, Meidong Lang

Shanghai Key Laboratory of Advanced Polymeric Materials, Key Laboratory for Ultrafine Materials of Ministry of Education, School of Materials Science and Engineering, East China University of Science and Technology, 130 Meilong Road, P. O. Box 391, Shanghai 200237, China

Correspondence to: Y. Zhang (E-mail: zhang.yan@ecust.edu.cn) or M. Lang (E-mail: mdlang@ecust.edu.cn)

**ABSTRACT:** Microsphere systems have been used to deliver drugs, proteins, and cells. However, dispersed microspheres can induce harmful effects after they are introduced into the body. To agglomerate these dispersed microspheres, an *in situ* forming system was developed to fabricate microsphere/hydrogel composites. Polycaprolactone microspheres with a porous surface and hollow core were physically incorporated into a genipin-crosslinked gelatin hydrogel. The incorporation of microspheres reduced the swelling capacities and weakened the unexpected volume expansion, which is not favorable for *in vivo* implants. Additionally, the reacted genipin ratio increased with increasing gelatin concentration. The degradation of the composite was also determined, and it was proposed that the degradation mechanism of the composite was bulk collapse, whereas that for the pure hydrogel was surface erosion. The obtained microsphere/hydrogel composite might have a great potential application as an injectable system for tissue regeneration. © 2012 Wiley Periodicals, Inc. *J. Appl. Polym. Sci.* 129: 689–698, 2013

**KEYWORDS:** biomedical applications; composites; degradation; gels

Received 14 May 2012; accepted 4 September 2012; published online 23 November 2012

**DOI:** 10.1002/app.38563

### INTRODUCTION

In recent years, the application of microspheres to the delivery of drugs and proteins has attracted great attention.<sup>1,2</sup> Hydrophobic drugs and hydrophilic proteins can be encapsulated in microspheres to obtain long-term sustained delivery.<sup>3–5</sup> In addition, the microspheres used as cell carriers show better cell attachment and growth.<sup>6,7</sup>

However, dispersed microspheres can readily induce chronic inflammation, foreign-body reaction, and fibrosis or thrombus after introduction to the human body.<sup>8,9</sup> Multiple approaches have been used to agglomerate dispersed microspheres; these include sintering by heating close to the melting temperature<sup>10</sup> and solvent-activated fusion.<sup>11,12</sup> However, these methods have poor repeatability, and the physical properties of the obtained composites cannot be well controlled. Moreover, the sintering treatment with a toxic solvent at high temperature tends to cause protein denaturation and cell death and might not be suitable for biomedical applications.<sup>12</sup>

Recently, a formulation method that overcomes these issues has been developed.<sup>13–15</sup> This method combines hydrogels with microspheres. The dispersed drug- or cell-loaded microspheres are introduced into a pregel solution first and then agglomer-

ated into a specific shape with gelation. This shape can be easily controlled to match the three-dimensional geometry of the damage sites for tissue generation.<sup>16</sup> More importantly, the incorporated microspheres can provide sufficient cell-affinitive interfaces to sustain long-term cell attachment and viability with common hydrogels.<sup>17,18</sup> In addition, researchers have found that hydrogel-system-based formulations can ameliorate undesirable drug-release behaviors (e.g., the inhibition of the initial burst).<sup>13,14</sup>

Gelatin, a partial derivative of collagen, has been recognized as an excellent biomaterial in tissue engineering.<sup>19–21</sup> A gelatin hydrogel can be crosslinked through various methods, including chemical reaction, UV irradiation, and physical entanglement, to enhance its mechanical properties and stability under aqueous conditions.<sup>22–24</sup> Previously, various kinds of microspheres, such as poly(lactide-co-glycolide) (PLGA) and dextran, have been incorporated into gelatin hydrogels for release.<sup>25–27</sup> However, the crosslinker that was used, glutaraldehyde, is toxic to biomolecules and cells; this limits the applications of these hydrogels in the biomedical field. Recently, a low-toxic and naturally occurring crosslinker, genipin, has been used to form gelatin hydrogels via the reaction of amino groups and the dihydropyran ring under neutral conditions.<sup>28</sup> Many researches have

indicated that genipin is more suitable for cell culturing compared to glutaraldehyde.<sup>28–31</sup> Genipin-crosslinked gelatin microspheres induce little inflammation when implanted *in vivo*<sup>32,33</sup> and can deliver growth factors while retaining their bioactivity.<sup>34</sup>

In this study, dispersed polycaprolactone (PCL) microspheres were introduced into a pregel gelatin solution. The solution was further crosslinked by genipin to obtain the microsphere/hydrogel composites. The effects of the microsphere size and gelatin concentration on the physical properties of the composites were thoroughly investigated. Their internal morphologies, reacted genipin contents, swelling abilities, and compressive moduli were determined. Furthermore, the degradation mechanism of the composites was studied. It was expected that the microsphere/hydrogel composite would have great potential application as an injectable system for tissue regeneration.

## EXPERIMENTAL

### Materials

$\epsilon$ -Caprolactone was provided by Sigma-Aldrich and was distilled over CaH<sub>2</sub> before use. Stannous octoate [Sn(Oct)<sub>2</sub>] and cyclotriphosphazene were supplied by Sigma-Aldrich Shanghai Trading Co., Ltd (Shanghai, China). Six-arm PCL (number-average molecular weight = 80,000 Da and polydispersity index = 1.66, as determined by gel permeation chromatography) was synthesized according to our previous study,<sup>35</sup> with cyclotriphosphazene as an initiator and Sn(Oct)<sub>2</sub> as a catalyst. Gelatin (BP, bloom  $\geq$  240) and poly(vinyl alcohol) (87–89% hydrolyzed, weight-average molecular weight =  $\sim$  74,800 Da) were purchased from Aladdin Reagent Co., Ltd. (Shanghai, China). Genipin (purity = 98%) was obtained from Shanghai Hotmed Sciences Co., Ltd. (Shanghai, China). All other reagents were analytical grade and were purchased from Sinopharm Chemical Reagent Co., Ltd (Shanghai, China).

### Fabrication of the PCL Microspheres

PCL microspheres with two sizes (small size =  $331 \pm 66 \mu\text{m}$  and large size =  $625 \pm 98 \mu\text{m}$ ) were fabricated according to a procedure in the literature with a slight modification.<sup>36</sup> Initially, a certain amount of PCL was dissolved in 7 mL of methylene chloride (10% w/v for the large microspheres and 6.67% w/v for the small microspheres). Then, a volume of 2.8 mL of an ammonium bicarbonate aqueous solution (15% w/v) was added to the PCL solution. The mixture was emulsified under magnetic stirring at room temperature for 30 min to obtain the first emulsion. Afterward, the first emulsion was poured into 300 mL of a poly(vinyl alcohol) aqueous solution (0.1% w/v). The mixture was stirred at room temperature at 400–500 rpm. After emulsification for 8 h, the solidified microspheres were collected via a screening mesh, washed with distilled water five times, and then lyophilized overnight.

### Fabrication of the Pure Gelatin Hydrogel

The respective gelatin solutions (10, 20, and 30 w/v) and genipin aqueous solution (1% w/v) were fully mixed with a volume ratio of 2 : 1. Then, the mixture was poured into a specific mold (10 mm in diameter and 15 mm in height) and incubated

**Table I.** Composition of the Composites

Code <sup>a</sup>	Microspheres used <sup>b</sup>	Gelatin concentration (%)
SH-10	Small	10
SH-20	Small	20
SH-30	Small	30
BH-10	Large	10
BH-20	Large	20
BH-30	Large	30
PH-10	N/A	10
PH-20	N/A	20
PH-30	N/A	30

N/A, not applicable.

<sup>a</sup>SH, BH, and PH represent gelatin hydrogels with small, large, and no microspheres, respectively. The number represents the gelatin concentration used, <sup>b</sup>Small microspheres:  $331 \pm 66 \mu\text{m}$ ; large microspheres:  $625 \pm 98 \mu\text{m}$ .

at 37°C for 8 h. The pure hydrogel without microspheres was finally obtained.

### Fabrication of the Microsphere/Hydrogel Composite

First, the PCL microspheres were prewetted over ethanol and incubated into double-distilled water. The microspheres absorbed water and sank to the bottom of the vial and were then taken out for further use. Subsequently, each gelatin solution (10, 20, and 30% w/v) was mixed with the genipin solution (1% w/v). The volume ratio of the gelatin to genipin solution was fixed at 2 : 1. The water-absorbing microspheres were added to the gelatin/genipin solution to obtain a microsphere concentration of 1 g/mL. The mixture was allowed to gel in a specific mold at 37°C for 8 h. The obtained composite was demolded and then freeze-dried for several days. All of the related data of the composites are listed in Table I. The samples were named and SH, BH, and PH represented gelatin hydrogels with small, large, and no microspheres, respectively.

### Characterization

The surfaces of the dried microspheres were observed with scanning electron microscopy (SEM; JSM-6360LV, JEOL, Tokyo, Japan). The microspheres were spread on an aluminum stub and coated with gold at 0.1 Torr. The SEM images were analyzed with Image J software (National Institutes of Health, Maryland, United State). The average microsphere diameters were calculated from the images with a sample size of at least 100 particles.

The cross-sectional microsphere was prepared by celloidin section technology. Briefly, a celloidin ethanol solution (18% w/v) was mixed with ethyl ether at a volume ratio of 1 : 1. Then, the microspheres were immersed into the solution and air-dried for 1–2 weeks to obtain a slab. The slab was freeze-sectioned and observed by SEM. The internal morphology of the composites was also determined by SEM. The dried microsphere/hydrogel composite was frozen and sectioned with a blade for SEM observation.

The reacted genipin ratio was determined with an ultraviolet-visible spectrophotometer (SP-725, Shanghai Spectrum Instrument Co., Ltd, Shanghai, China). Briefly, the dried composite was incubated in 20 mL of phosphate-buffered solution (PBS; pH 7.4) at 37°C with agitation (80 rpm). At selected time intervals, a volume of 5 mL of PBS was withdrawn from the medium and replaced with another 5 mL of fresh PBS. The test was conducted until no free genipin was detected in the medium. The genipin concentration was obtained on the basis of a comparison of the absorbance intensity at 230 nm with a standard calibration curve. The total free genipin content was calculated from the cumulative release of genipin. All of the experiments were performed in triplicate. The reacted genipin ratio was calculated as follows:

$$\text{Reacted genipin ratio (\%)} = (1 - \text{Free genipin content} / \text{Total genipin content}) \times 100\% \quad (1)$$

The swelling behavior was primarily induced by the gelatin hydrogel and was determined by a gravimetric method. The composite was immersed into a 25-mL beaker containing 10 mL of PBS at 37°C. At predetermined intervals, the composite was taken out, superficially wiped dry, and weighed. The swelling ratio was calculated as follows:

$$E_s(\%) = (W_s - W_d) / (W_d - W_m) \times 100\% \quad (2)$$

where  $E_s$  is the swelling ratio of the composites,  $W_d$  and  $W_s$  are the weight of the dried and the swollen composites at time  $t$ , respectively, and  $W_m$  is the weight of the microspheres. The experimental data were obtained from four different measurement.

The volume expansion of composite was determined by the volume ratio between the dried composite and the swollen one. A density bottle filled with ethanol was first weighed, and then, the dried composite was put into the density bottle. This caused a volume of ethanol to overflow. After the composite was removed, the density bottle was weighed again. This process was repeated for the composite swelled in water at 37°C for 24 h. The swollen composite was put into a density bottle filled with water. The density bottle was again weighed before and after it held the composite. The volume increment was calculated as follows:

$$\text{Volume ratio} = [(W_3 - W_4) / \rho_w] / [(W_1 - W_2) / \rho_e] \quad (3)$$

where  $W_1$  is the weight of the density bottle filled with ethanol,  $W_2$  is the weight of the density bottle with ethanol after holding the dried composite,  $W_3$  is the weight of the density bottle filled with water,  $W_4$  is the weight of the density bottle with water after holding the swollen composite, and  $\rho_w$  and  $\rho_e$  are the densities of water (1 g/mL) and ethanol (0.78 g/mL), respectively. The experimental data were obtained from four different measurement.

The compressive modulus analysis of the composite was conducted with an Instron machine (CMT5000, SANS, MTS Systems Corp., Shanghai, China) at ambient temperature and humidity. The crosshead speed and entrance force were set at 1 mm/min and 0.1 kN, respectively. The compressive modulus

value was determined by the initial linear slope (strain at 2–7%) of the stress–strain graph. The resulting data were evaluated with a paired  $t$  test. The experimental data were obtained from four different measurement.

#### Degradation Assay

The composite was incubated in 20 mL of PBS (pH 7.4) at 37°C for 10 days. At each time point, three independent samples were removed, freeze-dried, and weighed. The residual mass was calculated as follows:

$$\text{Residual mass(\%)} = W_t / W_0 \times 100\% \quad (4)$$

where  $W_0$  is the weight of the composites at the initial stage and  $W_t$  is the weight of the composites at time  $t$ . The removed samples were not used further to eliminate the error during the freeze-drying and reswelling process. The experimental data were obtained from four different measurement.

The gross morphology of the composite at time  $t$  was recorded by a digital camera (D80, Nikon).

## RESULTS AND DISCUSSION

### Size and Morphology of the Porous PCL Microspheres

In this study, the porous PCL microspheres were fabricated via a water-in-oil-in-water emulsion method with  $\text{NH}_4\text{HCO}_3$  as a porogen. We obtained the microspheres with two diameters by altering the PCL concentration; these were referred to as the large microspheres and small microspheres, respectively (Figure S1). Figure 1(A) illustrates the morphology of the small microspheres with a diameter of about  $331 \pm 66 \mu\text{m}$ . Many small pores with sizes of less than  $10 \mu\text{m}$  were observed on the surface [Figure 1(B)]. However, additional surface pores might be covered with a thin film. This could be attributed to the fact that the content of the oil phase ( $\text{CH}_2\text{Cl}_2$ ) for the small microspheres was higher than that for large microspheres. Because of the slower evaporation and longer time residence of the oil phase, a thin film might be formed on the surface of the microspheres. The cross section of the small microspheres, shown in Figure 1(C), indicated that a porous surface and hollow internality existed. The thickness of the porous wall was approximately  $50 \mu\text{m}$ , and the hollow core accounted for two-thirds of the microsphere volume. In addition, the outer surface was connected to the core through the open pore structure. The diameter of the microspheres increased when the polymer concentration was increased. The large microspheres had a diameter of  $625 \pm 98 \mu\text{m}$ , and the surface pores ( $20\text{--}30 \mu\text{m}$ ) were larger than those of the microspheres [Figure 1(D,E)]. A hollow core was also observed in the large microspheres, similar to the small microspheres, but the pore wall became thinner ( $\sim 15 \mu\text{m}$ ).

The PLGA-based microspheres were fabricated with a similar method.<sup>36</sup> However, the pore structure was significantly different from that of the PCL microspheres prepared here. An interconnective pore structure could be found on the PLGA microspheres, whereas the PCL microspheres exhibited a porous surface and hollow internality. We concluded that PCL was more hydrophobic than PLGA and exhibited less compatibility

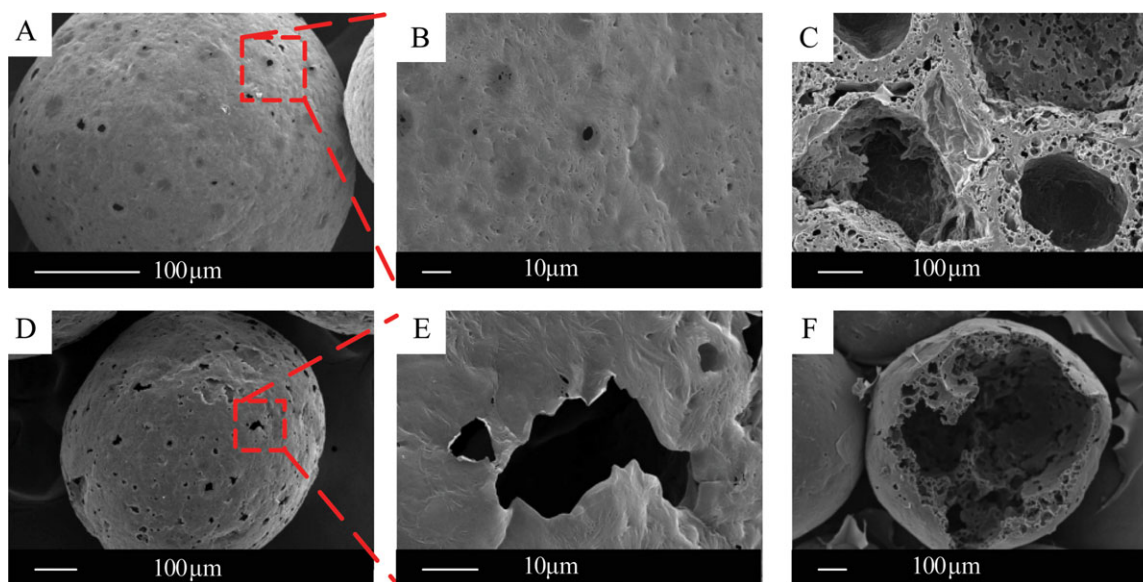


**Figure 1.** SEM images. (A,B) Small microspheres ( $331 \pm 66 \mu\text{m}$ ), (C) cross section of the small microspheres, (D,E) large microspheres ( $625 \pm 98 \mu\text{m}$ ), and (F) cross section of the large microspheres. [Color figure can be viewed in the online issue, which is available at [wileyonlinelibrary.com](http://wileyonlinelibrary.com).]

with water; thus, phase separation easily occurred in the first water/oil emulsion. After the addition of the first emulsion into the PVA solution, the water phase in the first emulsion quickly aggregated; this resulted in the formation of microspheres with a porous surface surrounding a hollow core.

It should be noted that this porous structure might be a prerequisite for cell culture. The porous surface could allow the swift exchange of the nutrition and waste as well as the ingrowth of cells (for the large microspheres). On the other hand, the hollow core could provide enough space for the cells to aggregate and communicate with other cells. The interaction among cells is considered to be very important in inducing the extracellular matrix secretion and the tissue formation.<sup>37,38</sup>

#### Evaluation of the Reacted Genipin Ratio

To gain a uniform distribution of PCL microspheres in the gelatin/genipin solution, the microspheres were initially prewetted. Afterward, the water-binding microspheres were mixed with the gelatin/genipin solution for gelling, and subsequently, a dark blue and white microsphere/hydrogel composite was obtained. Fourier transform infrared (FTIR) spectral analysis (Supporting Information, Figure S2) showed that the composite had a typical absorption band from PCL ( $\text{O}=\text{C}$ ,  $1705 \text{ cm}^{-1}$ ) and absorption bands corresponding to amide A, I, II, and III from gelatin.<sup>39</sup> The thermal analysis of differential scanning calorimetry (DSC, Q2000, TA Instrument, Delaware, United States) exhibited almost the same  $T_m$ 's as SH-10, BH-10, BH-30, and PCL (Figure S3); this indicated that the gelatin hydrogel, gelatin concentration, and microsphere diameter had little effect on the thermal properties of the composites.

A crosslinking reaction occurred between the amino groups of gelatin and the dihydropyran ring of genipin. The unreacted genipin could be detected by an ultraviolet–visible spectrophotometer and was used to evaluate the extent of the crosslinking

reaction.<sup>40,41</sup> As illustrated in Figure 2, for the PH, the reacted genipin ratio increased when the gelatin concentration increased ( $\text{PH-10} < \text{PH-20} < \text{PH-30}$ ). A similar trend was also observed for the composites ( $\text{SH-10} < \text{SH-20} < \text{SH-30}$ ;  $\text{BH-10} < \text{BH-20} < \text{BH-30}$ ). The results demonstrated that the extent of the crosslinking reaction improved with increasing gelatin concentration. In addition, the introduction of the porous microspheres had little effect on the gelatin–genipin crosslinking reaction. It was also indicated that the mobility of the genipin molecule was free and not inhibited by the microsphere suspension.

It has been reported that a safe dose of genipin is lower than  $0.5 \text{ mM}$ ,<sup>42</sup> and the highest genipin concentration among the samples (PH-10) reached only  $0.36 \text{ mM}$ . Thus, all of samples were in the range of a safe dose. Moreover, all of the samples could eliminate the free genipin from the bulk within 6 h after immersion in ethanol.

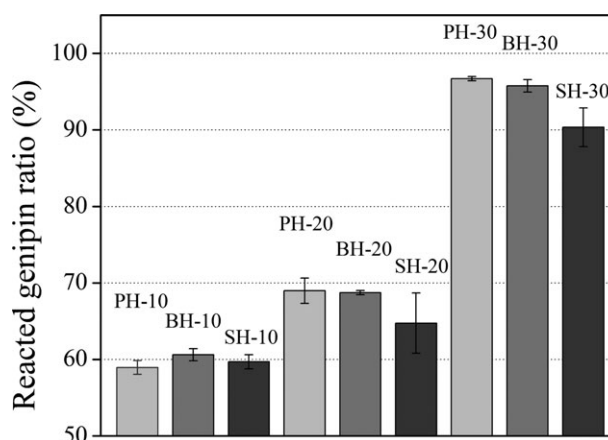


**Figure 2.** Reacted genipin ratio of the composites.

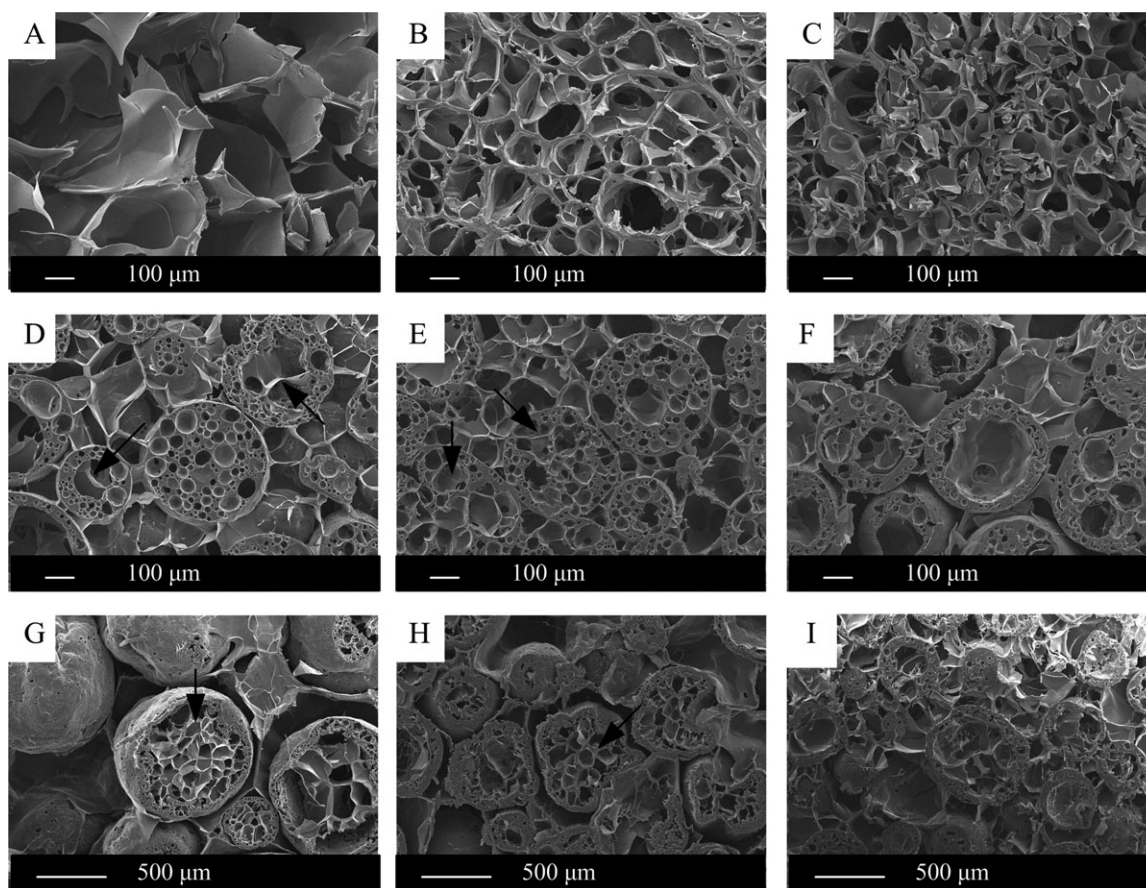


**Figure 3.** SEM images of the PH, SH, and BH composites: Morphologies of (A) PH-10, (B) PH-20, (C) PH-30, (D) SH-10, (E) SH-20, (F) SH-30, (G) BH-10, (H) BH-20, and (I) BH-30 (the arrow represented the gelation inside the microspheres).

### Internal Morphology of the PH, SH, and BH Composites

Figure 3 illustrates the internal morphologies of various gelatin hydrogels with and without PCL microspheres. PH-10 showed a loose internal structure with blurry and unfledged pore walls, whereas PH-20 and PH-30 exhibited regular and connective pore structures [Figure 3(A–C)]. The internal pore sizes of PH-10, PH-20, and PH-30 were measured to be  $421 \pm 74$ ,  $143 \pm 67$ , and  $121 \pm 27 \mu\text{m}$ , respectively. It was found that the pore size decreased when the gelatin concentration increased.

The morphologies of the composites containing small PCL microspheres (SH-10, SH-20, and SH-30) are illustrated in Figure 3(D–F). The internal pore sizes of the SH types were about  $100\text{--}200 \mu\text{m}$  [Figure 3(D–F)]. The gelatin concentration had no effect on the internal pore structure, unlike in the PH types. Meanwhile, the gelatin solution could penetrate the microspheres and gel inside the microspheres. Gelation inside the microspheres was observed for SH-10 and SH-20 but not for SH-30, as the 30% gelatin solution was too viscous to penetrate into the microspheres.

The internal pore sizes in the BH types ( $>600 \mu\text{m}$ ) were larger than those in the SH types [ $100\text{--}200 \mu\text{m}$ ; Figure 3(G–I)]. It was believed the larger microsphere significantly inhibited the gelling process. Internal gelation was more readily observed in the BH-type large microspheres than in the SH-type small microspheres,

as shown in Figure 1, because of the more porous surfaces of the large microspheres.

### Swelling Ratio of the Composites

The incorporated microspheres and gelatin concentration greatly influenced the swelling ratio of the composites. As shown in Figure 4, all of the PH types were rapidly swollen; for example, the swelling ratio of PH-20 was about 20 times the weight in the dried state after 48 h of immersion. By comparison with PH-10, PH-20, and PH-30, it was found that a higher gelatin content resulted in a higher swelling ratio. The swelling abilities of PH-20 and PH-30 were 1.6 and 1.4 times higher than that of PH-10. However, no distinct difference was found among the BH types. In addition, the swelling ratios of the SH types decreased with increasing gelatin concentration.

The swelling ability of the gelatin hydrogel was inhibited after the incorporation of microspheres. For a given gelatin concentration, such as 20%, the swelling ratios of SH-20 and BH-20 were 2.8 and 1.5 times lower than that of PH-20. The decrease was greater on SH-20 than that on BH-20. This could be attributed to the fact that the quantity of the small microspheres ( $331 \pm 66 \mu\text{m}$ ) was greater than that of the large microspheres ( $625 \pm 98 \mu\text{m}$ ) for the same weight; this led to a stronger restriction on the swelling of gelatin chain. In addition, the SH types exhibited the opposite trend in comparison with the PH

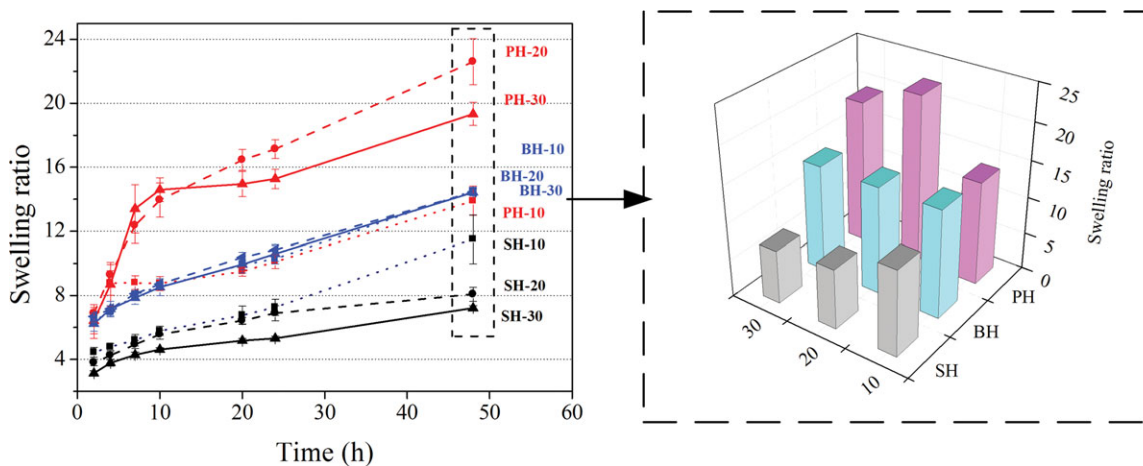


**Figure 4.** Swelling ratios of the PH, SH, and BH types as a function of time. [Color figure can be viewed in the online issue, which is available at [wileyonlinelibrary.com](http://wileyonlinelibrary.com).]

types with regard to the effect of the gelatin concentration. This suggested that the incorporated microspheres occupied the space inside the composites and squeezed the free room for chain swelling. Thus, the higher gelatin concentration had less free space and induced a greater inhibition of the swelling ability.

#### Volume Expansion of the Composite

The inhibition on the swelling ratio resulted in a decrease in the volume expansion. After it was incubated in water for 24 h, the volume of the pure hydrogel expanded to some extent [Figure 5(A,B)]. For PH-30, the volume of the swollen hydrogel was nearly six times larger than that of the dried hydrogel, whereas

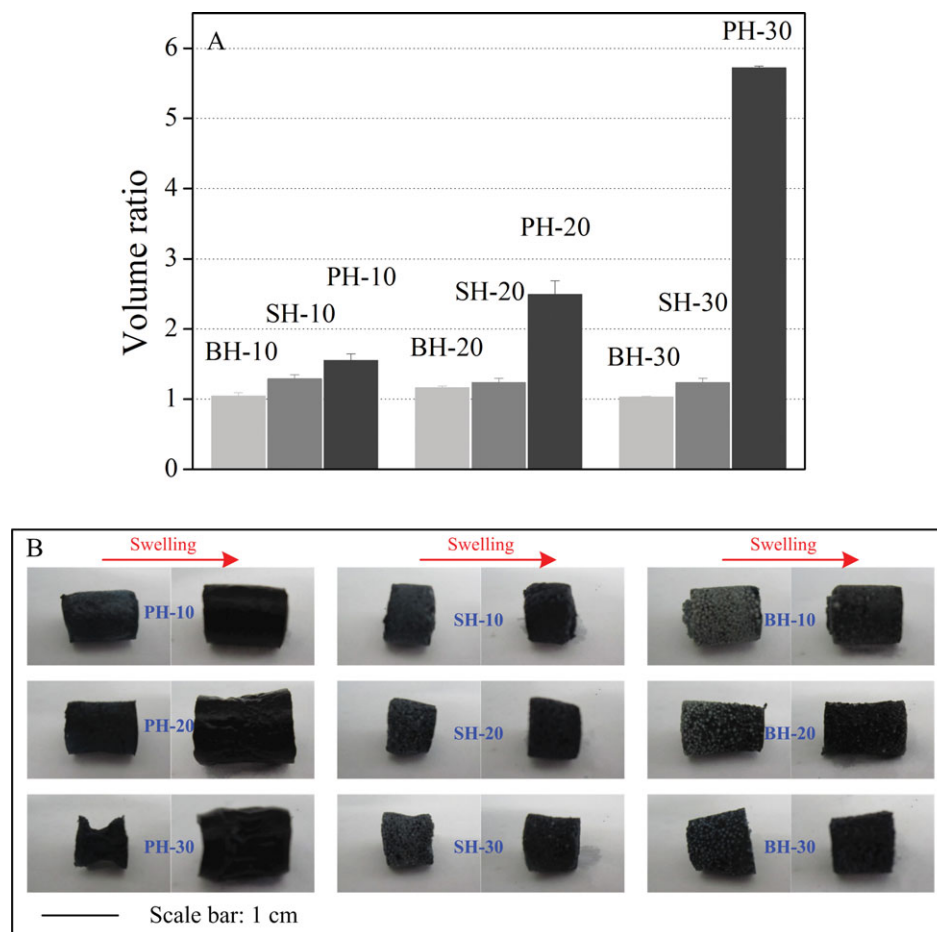


**Figure 5.** (A) Volume ratio between the swollen samples and the dried samples and (B) digital images of the volume expansion of the PH, SH, and BH types. [Color figure can be viewed in the online issue, which is available at [wileyonlinelibrary.com](http://wileyonlinelibrary.com).]

after the incorporation of the microspheres, the volume change in the composite was slight [Figure 5(A,B)].

Unexpected volume expansion might be not favorable for *in vivo* application, and a stable dimension of the implant should be required for high success in tissue regeneration.<sup>43</sup> Here, it was important that the incorporation of the microspheres in the composite hydrogel restricted unexpected volume expansion and maintained stable dimensions.

### Mechanical Properties of PH, SH, and BH

The compressive moduli of all of the samples exhibited a dependence on gelatin concentration (Figure 6). For the PH types, PH with a higher gelatin concentration had a denser network [Figure 3(A–C)], and this led to a stronger compressive resistance.

After the introduction of the microspheres, the compressive moduli decreased. This might have been due to the disruption of the gelatin network. The incorporated microspheres destroyed the longitudinal continuity of the connective structure and induced a decrease in the mechanical integrity. The small microspheres had larger quantities than the large ones under the same weight, and thereby, the decrease was greater in SH than in BH.

### Degradation Properties of the PH, SH, and BH Types

The degradation assay was conducted in PBS (pH 7.4) at 37°C for 10 days. The changes in mass and gross morphology were determined as a function of time during the degradation process (Figures 7 and 8). For the PH types, the mass losses of PH-30, PH-20, and PH-10 were 30.3, 45.2, and 56.8%, respectively, after 10 days [Figure 7(A)]. This was attributed to the gradual disintegration of the crosslinking point and the dissolution of the unzipped free gelatin. Relatively slow erosion could be obtained with a high gelatin concentration because of the dense network.

After the incorporation of PCL microspheres, the effect of the gelatin concentration on SH and BH was opposite to that on the PH types. Figure 7(B) shows that SH-10 experienced slight degradation, whereas SH-30 totally collapsed (Figure 8). Similar trends were also observed for the BH types [Figure 7(C)]. This

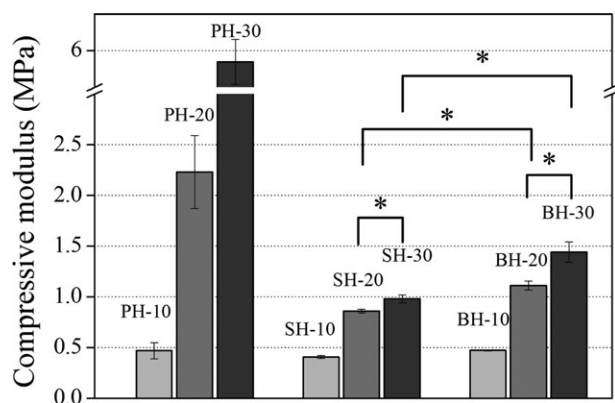


**Figure 6.** Compressive moduli of the PH, SH, and BH types. The asterisk represents a *p* value of less than 0.05 between two groups.

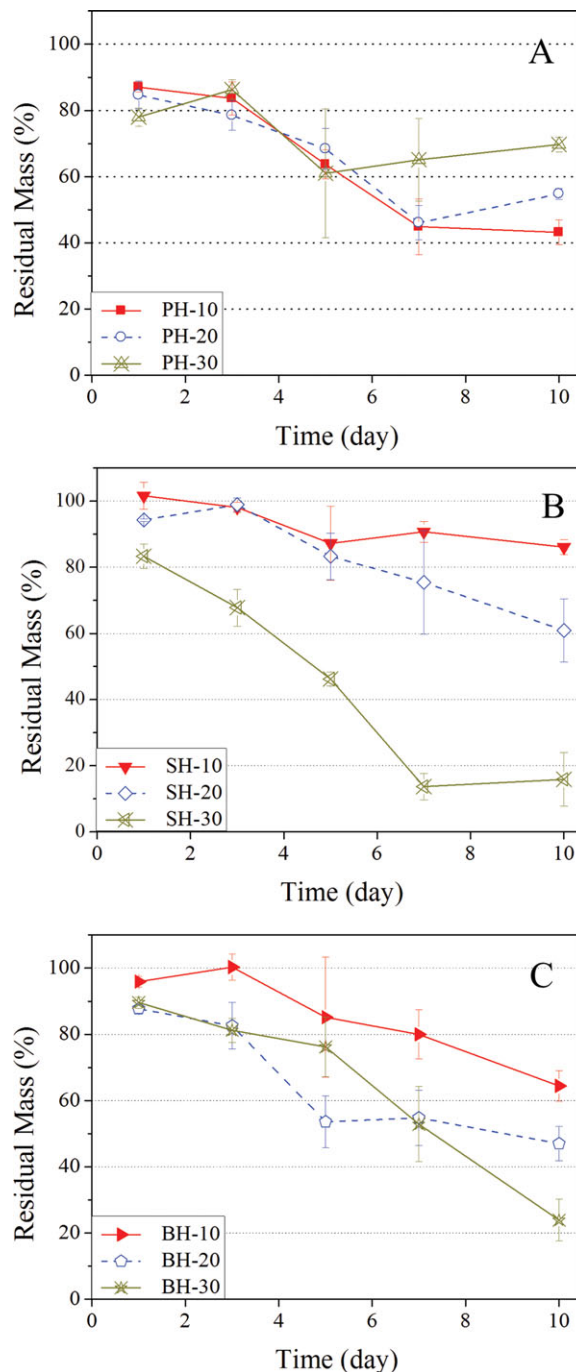


**Figure 7.** Degradation assay of the PH, SH, and BH types as a function of time: mass loss of (A) PH, (B) SH, and (C) BH. [Color figure can be viewed in the online issue, which is available at [wileyonlinelibrary.com](http://www.wileyonlinelibrary.com).]

was ascribed to the different degradation mechanisms for the PH, SH, and BH types.

The degradation mechanism is described in Figure 9. The dimensions of PH reduced in a stepwise manner, with surface erosion occurring in bulk. A higher gelatin concentration resulted in bulks that took more time to dissolve because of their denser internal structure. Thus samples with less dense

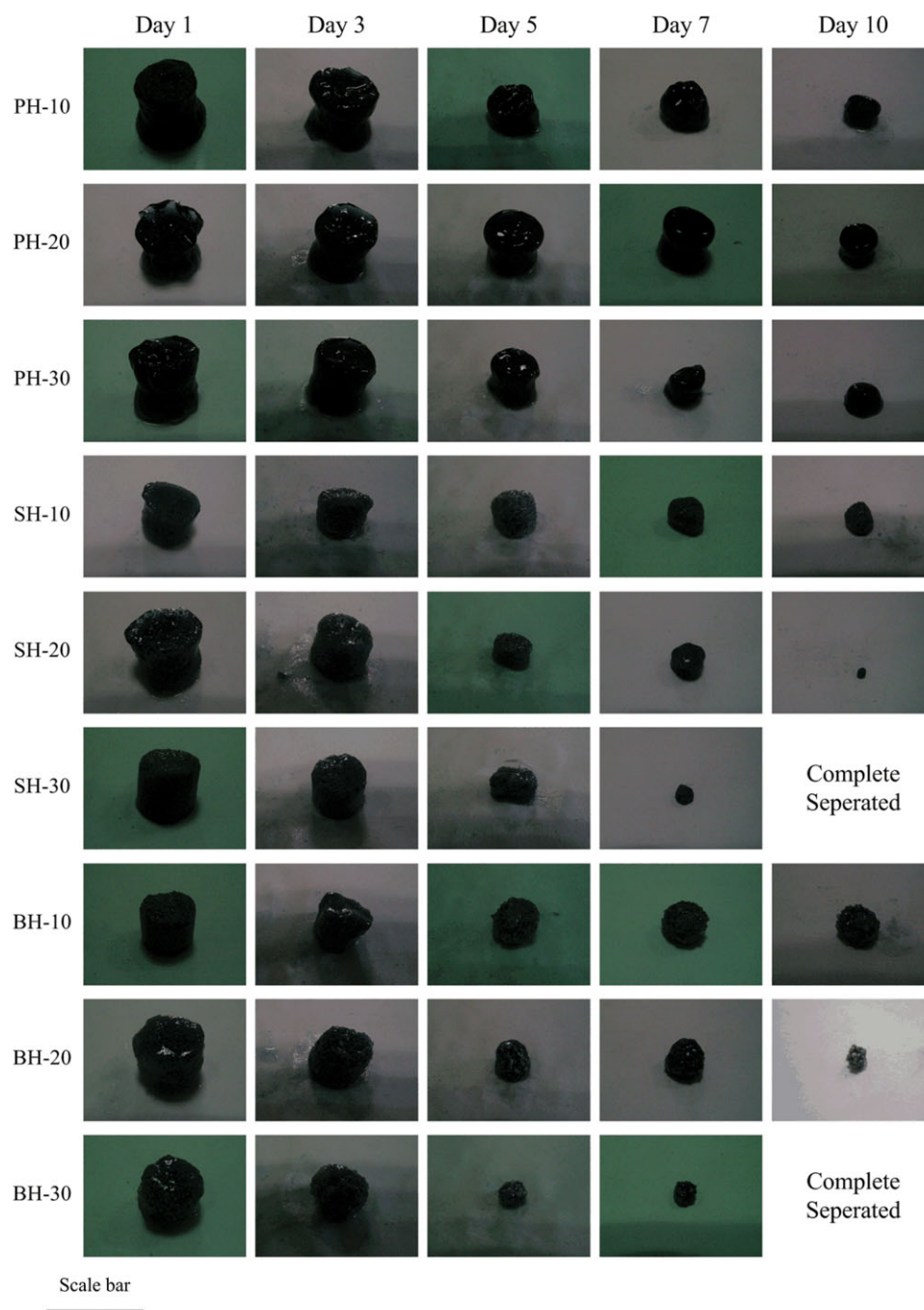


**Figure 8.** Digital images of the PH, SH, and BH types during degradation (scale bar = 20 mm). [Color figure can be viewed in the online issue, which is available at [wileyonlinelibrary.com](http://wileyonlinelibrary.com).]

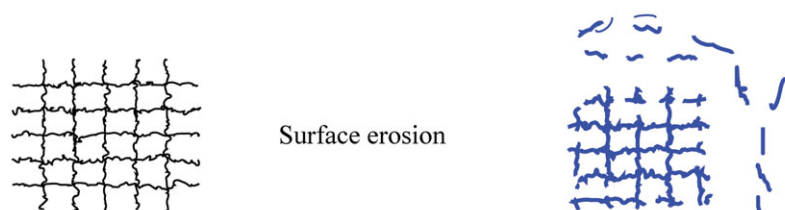
structures, PH-10, disintegrated more quickly than the more dense samples, PH-20 and PH-30.

The degradation mechanisms of the SH and BH types were considered to be bulk collapse. The repulsions between the hydrogel and the microspheres were responsible for the dimensional reduction of the SH and BH types. As shown in Figure 4, the incorporated microspheres restrained the swelling ability of the gelatin hydrogel. In the case of low gelatin concentrations (SH-10 and BH-10), the relatively loose structure provided enough space for the hydrated chains to extend. The additional

free space diminished the interaction between the hydrogel and the microspheres. However, at a high gelatin concentration (SH-30 and BH-30), the internal structure was more compact. When the gelatin was swollen, the network became dense and squeezed the nearby microspheres. As the interaction enhanced, the composite disintegrated into small chunks of microspheres and hydrogel in a stepwise manner. Therefore, the erosion of the hydrogel resulted in rapid mass and volume reductions, and both SH-30 and BH-30 were completely disintegrated in 10 days (Figure 8).



Pure hydrogel:



Microsphere/hydrogel composites:

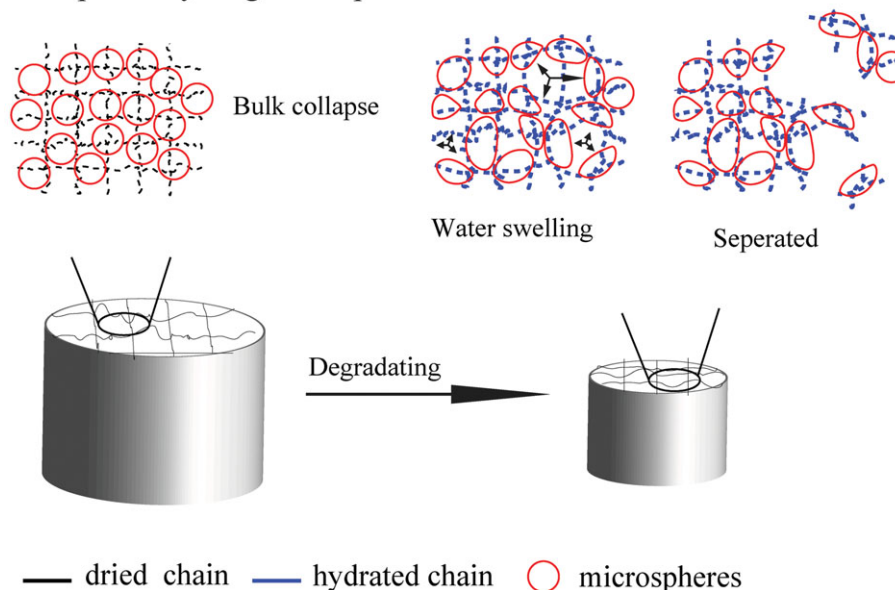


**Figure 9.** Degradation mechanism of the pure hydrogel and the microsphere/hydrogel composites. [Color figure can be viewed in the online issue, which is available at [wileyonlinelibrary.com](http://wileyonlinelibrary.com).]

This composite had good biocompatibility (cells could proliferate in a sustained way in the composite, as shown in the Supporting Information, Figures S4 and S5) and has great potential application as injectable implants for tissue regeneration. When the cell-loaded microspheres are applied, the composite could be injected and formed *in situ* at the defect site. The degradation study indicated that the composite could not be cultured *in vitro* for a long time because of the rapid bulk collapse. However, the unique degradation behavior might be helpful for *in vivo* application. Supposedly, after the composite was implanted *in vivo*, amounts of space would be induced from the bulk collapse inside the damaged site. Then, the cells had sufficient space to proliferate and freely migrate. The space would also permit the settlement of the extracellular matrix and accelerate tissue formation.

## CONCLUSIONS

We successfully agglomerated porous PCL microspheres into a gelatin/genipin hydrogel. The physicochemical properties of the composites were influenced by the incorporation of the PCL microspheres. The geometrical shape of the composites could easily be maintained after water swelling compared to PH. The composites also exhibited bulk collapse, which might improve

the quality of tissue formation. The PCL microsphere/gelatin hydrogel composite could have great potential application as an injectable implant for tissue regeneration.

## ACKNOWLEDGMENT

This research was supported by the Fundamental Research Funds for the Central Universities (WD0913008, WD1014036), the National Natural Science Foundation of China (20804015), Shu Guang Project of Shanghai Municipal Education Commission, Specialized Research Fund for the Doctoral Program of Higher Education (200802511021), the Natural Science Foundation of Shanghai (08ZR1406000), and the Program for Changjiang Scholars and Innovative Research Team in University (IRT0825).

## REFERENCES

- Oliveira, M. B.; Mano, J. F. *Biotechnol. Prog.* **2011**, *27*, 897.
- Martin, Y.; Eldardiri, M.; Lawrence-Watt, D. J.; Sharpe, J. R. *Tissue Eng. B* **2010**, *17*, 71.
- Baimark, Y.; Srisa-Ard, M. *J. Appl. Polym. Sci.* **2012**, *124*, 3871.

4. Fenández, A.; Teijón, C.; Benito, M.; Iglesias, I.; Lozano, R.; Teijón, J. M.; Blanco, M. D. *J. Appl. Polym. Sci.* **2012**, *124*, 2987.
5. Tan, G.; Liao, J.; Ning, C.; Zhang, L. *J. Appl. Polym. Sci.* **2012**, *125*, 3509.
6. Shin, U. S.; Park, J. H.; Hong, S. J.; Won, J. E.; Yu, H. S.; Kim, H. W. *Mater. Lett.* **2010**, *64*, 2261.
7. Hong, S.-J.; Yu, H.-S.; Kim, H.-W. *Macromol. Biosci.* **2009**, *9*, 639.
8. Tran, V.-T.; Benoît, J.-P.; Venier-Julienne, M.-C. *Int. J. Pharm.* **2011**, *407*, 1.
9. Anderson, J. M.; Shive, M. S. *Adv. Drug Delivery Rev.* **1997**, *28*, 5.
10. Luciani, A.; Coccoli, V.; Orsi, S.; Ambrosio, L.; Netti, P. *Biomaterials* **2008**, *29*, 4800.
11. Shi, X.; Su, K.; Varshney, R. R.; Wang, Y.; Wang, D. A. *Pharm. Res.* **2011**, *28*, 1224.
12. Jaklenec, A.; Hinckfuss, A.; Bilgen, B.; Ciombor, D.; Aaron, R.; Mathiowitz, E. *Biomaterials* **2008**, *29*, 1518.
13. Lee, J.; Lee, K. *Macromol. Biosci.* **2009**, *9*, 671.
14. Patel, Z.; Ueda, H.; Yamamoto, M.; Tabata, Y.; Mikos, A. *Pharm. Res.* **2008**, *25*, 2370.
15. Wang, Y.; Wei, Y. T.; Zu, Z. H.; Ju, R. K.; Guo, M. Y.; Wang, X. M.; Xu, Q. Y.; Cui, F. Z. *Pharm. Res.* **2011**, *28*, 1406.
16. Van Tomme, S. R.; Storm, G.; Hennink, W. E. *Int. J. Pharm.* **2008**, *355*, 1.
17. Wang, C.; Varshney, R.; Wang, D. *Adv. Drug Delivery Rev.* **2010**, *62*, 699.
18. Wang, C.; Gong, Y.; Zhong, Y.; Yao, Y.; Su, K.; Wang, D. A. *Biomaterials* **2009**, *30*, 2259.
19. Lin, Y.; Chen, X.; Jing, X.; Jiang, Y.; Su, Z. *J. Appl. Polym. Sci.* **2008**, *109*, 530.
20. Yang, C.; Wu, X.; Zhao, Y.; Xu, L.; Wei, S. *J. Appl. Polym. Sci.* **2011**, *121*, 3047.
21. Zhao, J.; Zhao, Y.; Guan, Q.; Tang, G.; Zhao, Y.; Yuan, X.; Yao, K. *J. Appl. Polym. Sci.* **2011**, *119*, 786.
22. Nichol, J. W.; Koshy, S. T.; Bae, H.; Hwang, C. M.; Yamanlar, S.; Khademhosseini, A. *Biomaterials* **2010**, *31*, 5536.
23. Lien, S.; Ko, L.; Huang, T. *Acta Biomater.* **2009**, *5*, 670.
24. Linh, N. T. B.; Min, Y. K.; Song, H. Y.; Lee, B. T. *J. Biomed. Mater. Res. B* **2010**, *95*, 184.
25. Kempen, D. H. R.; Lu, L.; Hefferan, T. E.; Creemers, L. B.; Maran, A.; Classic, K. L.; Dhert, W. J. A.; Yaszemski, M. J. *Biomaterials* **2008**, *29*, 3245.
26. Chen, F.; Zhao, Y.; Sun, H.; Jin, T.; Wang, Q.; Zhou, W.; Wu, Z.; Jin, Y. *J. Controlled Release* **2007**, *118*, 65.
27. Huang, S.; Zhang, Y.; Tang, L.; Deng, Z.; Lu, W.; Feng, F.; Xu, X.; Jin, Y. *Tissue Eng. Part A* **2009**, *15*, 2617.
28. Muzzarelli, R. *Carbohydr. Polym.* **2009**, *77*, 1.
29. Huang, Z.; Yu, B.; Feng, Q.; Li, S.; Chen, Y.; Luo, L. *Carbohydr. Polym.* **2011**.
30. Karnchanajindanun, J.; Srisa-Ard, M.; Baimark, Y. *Carbohydr. Polym.* **2011**, *85*, 674.
31. Liang, H.-C.; Chang, W.-H.; Liang, H.-F.; Lee, M.-H.; Sung, H.-W. *J. Appl. Polym. Sci.* **2004**, *91*, 4017.
32. Liang, H.-C.; Chang, W.-H.; Lin, K.-J.; Sung, H.-W. *J. Biomed. Mater. Res. A* **2003**, *65*, 271.
33. Wei, H.-J.; Yang, H.-H.; Chen, C.-H.; Lin, W.-W.; Chen, S.-C.; Lai, P.-H.; Chang, Y.; Sung, H.-W. *J. Controlled Release* **2007**, *120*, 27.
34. Solorio, L.; Zwolinski, C.; Lund, A. W.; Farrell, M. J.; Stegeman, J. P. *J. Tissue Eng. Regen. Med.* **2010**, *4*, 514.
35. Huang, X.; Xiao, Y.; Lang, M. *Macromol. Res.* **2011**, *19*, 113.
36. Kim, T.; Yoon, J.; Lee, D.; Park, T. *Biomaterials* **2006**, *27*, 152.
37. Rossello, R.; Kohn, D. *J. Biomed. Mater. Res. B* **2009**, *88*, 509.
38. Bryant, D.; Mostov, K. *Nat. Rev. Mol. Cell Biol.* **2008**, *9*, 887.
39. Panzavolta, S.; Gioffrè, M.; Focarete, M. L.; Gualandi, C.; Foroni, L.; Bigi, A. *Acta Biomater.* **2011**, *7*, 1702.
40. Nickerson, M.; Patel, J.; Heyd, D.; Rousseau, D.; Paulson, A. *Int. J. Biol. Macromol.* **2006**, *39*, 298.
41. Mi, F.; Shyu, S.; Peng, C. *J. Polym. Sci. Part A: Polym. Chem.* **2005**, *43*, 1985.
42. Wang, C.; Lau, T. T.; Loh, W. L.; Su, K.; Wang, D. A. *J. Biomed. Mater. Res. B* **2011**, *97*, 58.
43. Chen, Y.; Chang, J.; Cheng, C.; Tsai, F.; Yao, C.; Liu, B. *Biomaterials* **2005**, *26*, 3911.